Journal of Materials Science Research; Vol. 4, No. 1; 2015
ISSN 1927-0585 E-ISSN 1927-0593
Published by Canadian Center of Science and Education

Two-Stage Approach for Improving the Thickness Distribution in Superplastic Forming

Reem A. Jafar[1], Firas S. Jarrar[2] & Naser S. Al-Huniti[1]

[1] Department of Mechanical Engineering, The University of Jordan, Amman, Jordan

[2] Department of Mechanical Engineering, The Petroleum Institute, Abu Dhabi, United Arab Emirates

Correspondence: Firas S. Jarrar, Department of Mechanical Engineering, The Petroleum Institute, P.O. Box 2533, Abu Dhabi, United Arab Emirates. Tel: 971-2607-5018. E-mail: fjarrar@pi.ac.ae

Received: October 31, 2014 Accepted: November 3, 2014 Online Published: November 9, 2014

doi:10.5539/jmsr.v4n1p12 URL: http://dx.doi.org/10.5539/jmsr.v4n1p12

Abstract

Superplastic Forming (SPF) process has many unique advantages over conventional forming operations including ability to produce complex thin shapes and significant cost and weight savings potentials. However, the SPF may result in excessive thinning at certain locations and a non-uniform thickness profile. To address these issues, the two-stage SPF process was developed to improve the uniformity of thickness distribution. In this work, two techniques were considered to improve the final thickness distribution of a complex shape, namely, the license plate pocket potion of an automobile decklid outer panel. These two techniques are the reverse free bulging and sheet preforming. The commercial finite element code, ABAQUS^{TM}, was used to model the two-stage SPF process of an aluminum alloy AA5083 sheet at 450 °C. The study concluded that reverse free bulging did not result in improvements in the thickness profile compared with that obtained from the single-stage SPF. However, the sheet preforming technique, with an engineered preform cavity, resulted in an almost uniform thickness distribution for the superplastically formed part.

Keywords: superplastic forming, two stage forming, preform cavity, AA5083

1. Introduction

Superplasticity is the ability of certain type of materials to exhibit large tensile deformation prior to fracture. While the maximum elongation prior to failure that can be achieved in conventional alloys does not exceed 120%, superplastic materials have the capability to exhibit very large elongations, i.e. >500%, (Pilling & Ridley, 1989). The conditions for superplasticity to occur are forming within a specific range of strain rates, and forming in narrow ranges of temperatures (Pilling & Ridley, 1989). Each material has a unique optimum value of strain rate, and a narrow temperature range which lies above half the material's absolute melting point.

The SPF process is carried out by placing a sheet of superplastic material on a pre-heated single-sided die. The sheet is heated to the required SPF temperature which is specified for that material. Then, an inert gas is applied to one side of the sheet to control the rate of deformation and force the sheet to take the shape of the die cavity.

As a manufacturing process, SPF offers many unique advantages over conventional forming techniques including greater design flexibility, low dies cost, the elimination of spring back, and producing components with complex geometries in one manufacturing step (Kleiner, Geiger, & Klaus, 2003). Accordingly, SPF reduces or eliminates the sub-components and joining operations. In addition, SPF allows for the satisfactory forming of lightweight alloys, which opens the door for substituting steel with lighter weight alloys for automotive components. This would have a huge effect on energy consumption and environment.

The main limitation of SPF is the slow nature of this process compared to other forming operations. Other limitations include the non-uniformity of the produced part thickness, the possibility of severe thinning and necking at certain locations and large amounts of cavities developed in some superplastic alloys, see for example (Jarrar, Liewald, Schmid, & Fortanier, 2014).

An interesting approach to improve the thickness profile of superplastically formed parts is preforming. It was concluded by (Johnson, Al-Naib, & Duncan, 1972) that multistage operations that take advantage of the high friction conditions of SPF were the most effective at producing improved thickness uniformity. Few researchers studied the effect of preforming; (Nakamura, 1989) and (Fischer, 1998) used the preform technique in their works to form simple

geometries. In a more recent study (Luckey, Friedman, & Weinmann, 2009), a two-stage SPF process was developed, based on the inventions of (Nakamura, 1989) and (Fischer, 1998). Gas pressure was used to form the blank into a preform die cavity prior to the pressure being reversed to form the sheet into the final component cavity. The preform had been designed to improve the forming of a complex component by providing a superior thickness profile as compared to a single stage forming cycle. Their work was based on finite element analysis and experimental iterations, and focused mainly on the effect of the length of line of the preform cavity.

Abu-Farha and Nazzal (2010) imposed a pre-thinning reverse bulging step before the forward SPF stage. Their results showed that the reverse free bulging approach improved the thickness profile and decreased the severe thinning with specific part geometries and materials. Recently, Lan, Fuh, Lee, Chu, and Chang (2013) used two-stage SPF to form a deep and irregular trough. The sheet was initially bent into a V-shaped groove prior to the gas forming work. They found that preforming of the V blank creates a uniform length of line and improved the thickness profile of the final part. However, a serious wrinkling situation was encountered in their study.

Our main goal is to consider the effect of the shape of the preform cavity on final thickness distribution of the part, and attempt to find an engineered shape for better thickness distribution. We will develop a finite element method predictive tool of the process and suggest certain process guidelines that would overcome some of the limitations of the SPF process.

2. Constitutive Model

A superplastic aluminum alloy sheet, AA5083, was used in this work which had a nominal thickness of 1.2 mm. The constitutive model used to describe the superplastic deformation here is the power law equation:

$$\sigma = k\dot{\varepsilon}^m\varepsilon^n \tag{1}$$

where σ is the effective flow stress, $\dot{\varepsilon}$ is the effective strain rate, m is the strain rate sensitivity exponent, n is the strain hardening exponent, and k is the strength coefficient. The values of k, m and n were determined by fitting the model to tensile tests taken from (Krajewski and Montgomery, 2004). The obtained values of k, m and n are shown in Table 1.

Table 1. The obtained m, n, and k values for the constitutive model

k	**m**	**n**
253.89	0.37	0.29

The developed constitutive model was verified by comparing its results with analytical results and experimental data for bulging a sheet with an original thickness of 1.2 mm to form a hemisphere with a radius of 57 mm. The following equations, taken from (Dutta and Mukherjee, 1992) were used to find the analytical results of the radius of curvature, the pole thickness, and the pressure profile, respectively:

$$\rho = \frac{a}{2[\exp(-\dot{\varepsilon}t)(1-\exp(-\dot{\varepsilon}t))]^{1/2}} \tag{2}$$

$$\frac{S}{\rho} = \frac{2S_0\exp(-\dot{\varepsilon}t)[\exp(-\dot{\varepsilon}t)(1-\exp(-\dot{\varepsilon}t))]^{1/2}}{a} \tag{3}$$

$$P = 4\frac{S_0}{a}\sigma\exp(-\dot{\varepsilon}t)[\exp(-\dot{\varepsilon}t)(1-\exp(-\dot{\varepsilon}t))]^{\frac{1}{2}} \tag{4}$$

where ρ is the radius of curvature, a is the radius of the die, $\dot{\varepsilon}$ is the effective strain rate, S is the thickness after time t, S_0 is the original sheet thickness, σ is the effective flow stress, and P is the applied pressure.

The pole height was found by using the following relationship relating the radius of curvature, ρ, and the height, h, taken from Jovane (1968):

$$\rho = \frac{a^2+h^2}{2h} \tag{5}$$

Two sets of finite element (FE) simulation runs were performed. In the first set, a constant gas pressure was prescribed during bulge forming. In the second set, the gas pressure profile was computed (rather than prescribed at the outset of the simulation) using an algorithm internal to ABAQUS™. Simulation results for constant gas pressure were compared with experimental AA5083 data from bulge tests taken from (Bradley, 2004). Figures

1(a-b) show the FE predicted dome pole height at the two gas pressures (solid curves). The triangles correspond to the experimental data. Figures 2(a-b) show the dome pole thickness evolution at the same pressures considered in Figure 1. Figures 1 and 2 show that the developed material model leads to FE predictions that follow the experimental trends. ABAQUS™ results for constant strain rate forming were compared with the analytical results. Figure 3 shows the FE predicted dome pole height at a strain rate of 0.0005 1/sec (solid curve), the triangles correspond to the analytical results. Figure 4 shows the dome pole thickness evolution at the same strain rate considered in Figure 3. Figures 3 and 4 show that the developed material model leads to FE predictions that follow the analytical trends.

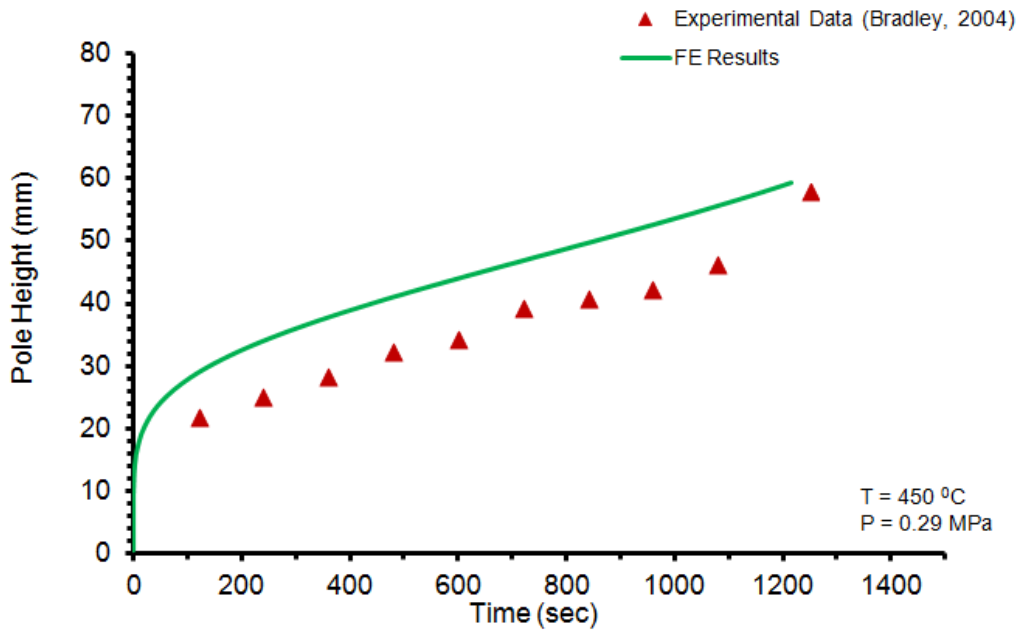

(a)

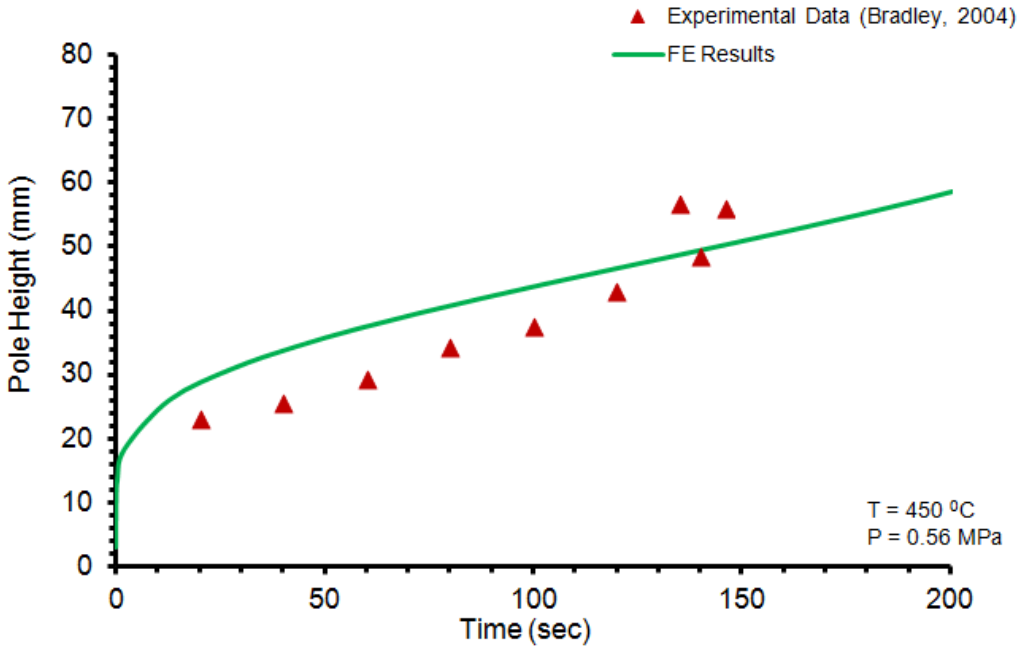

(b)

Figure 1. Dome pole height for AA5083 at 450 °C for FE model (solid line) and experiment data (triangles) (Bradley, 2004): (a) 0.29 MPa (42 psi), and (b) 0.56 MPa (81 psi)

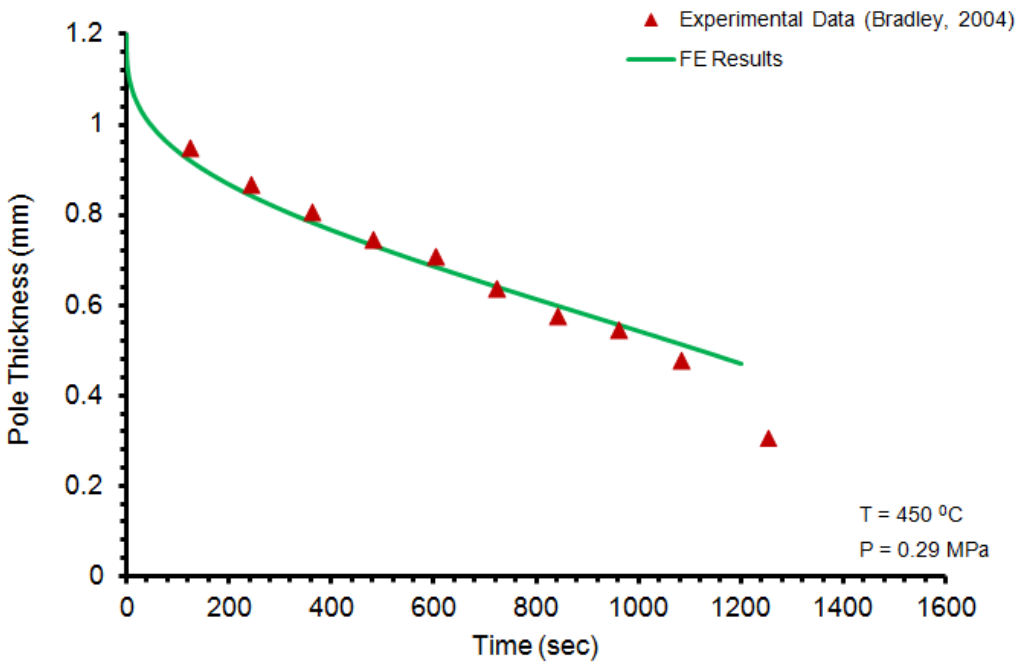

(a)

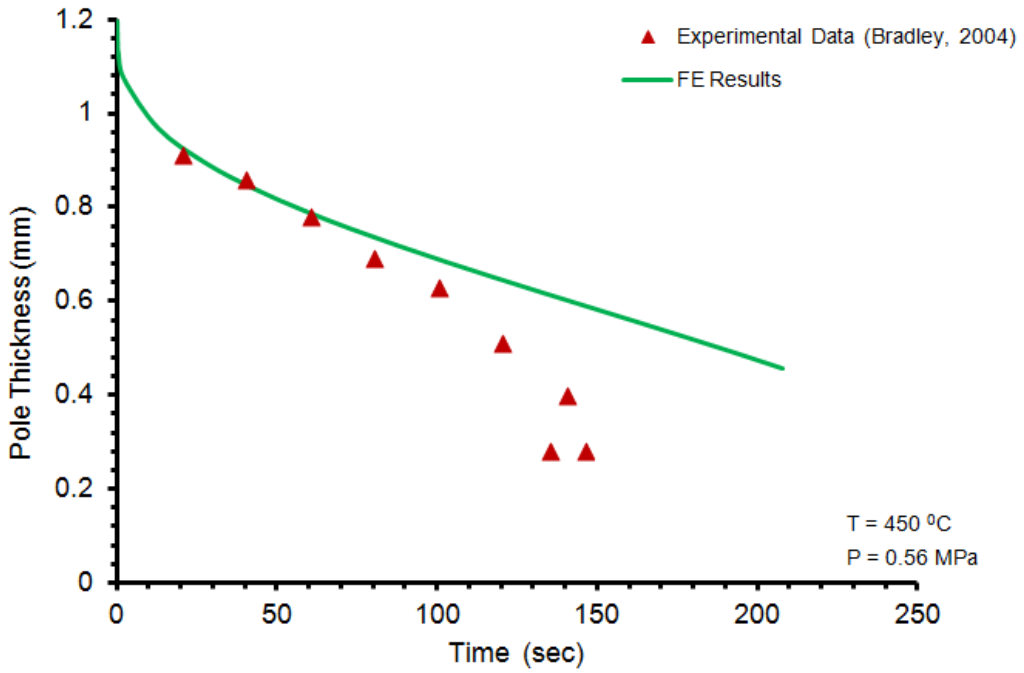

(b)

Figure 2. Dome pole thickness for AA5083 at 450 °C for FE models (solid lines) and experimental data (triangles) (Bradley, 2004): (a) 0.29 MPa (42 psi), and (b) 0.56 MPa (81 psi)

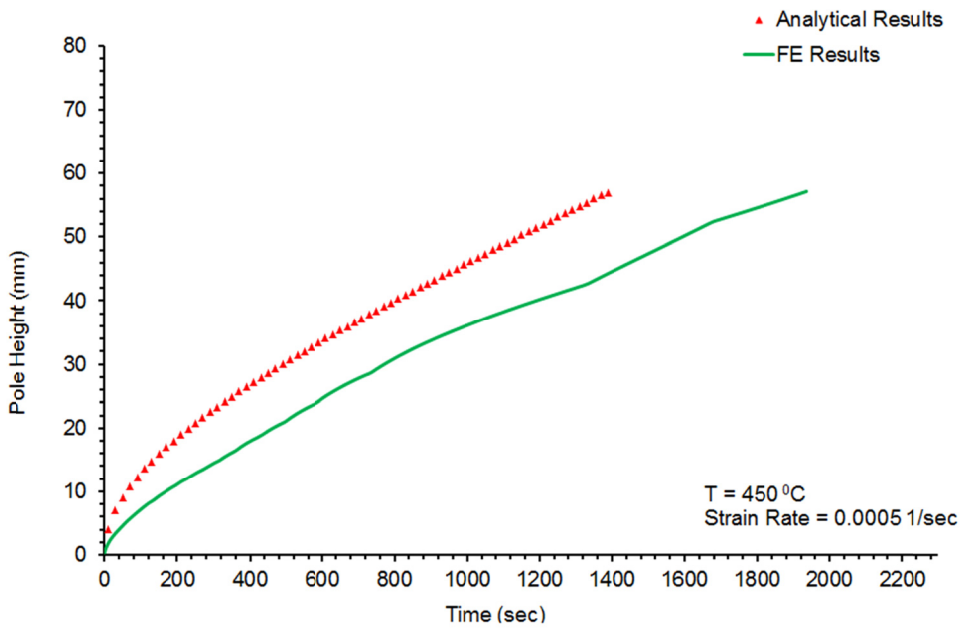

Figure 3. Dome pole height for AA5083 at 450 °C for FE model (solid line) and analytical results (triangles) (Dutta and Mukherjee, 1992)

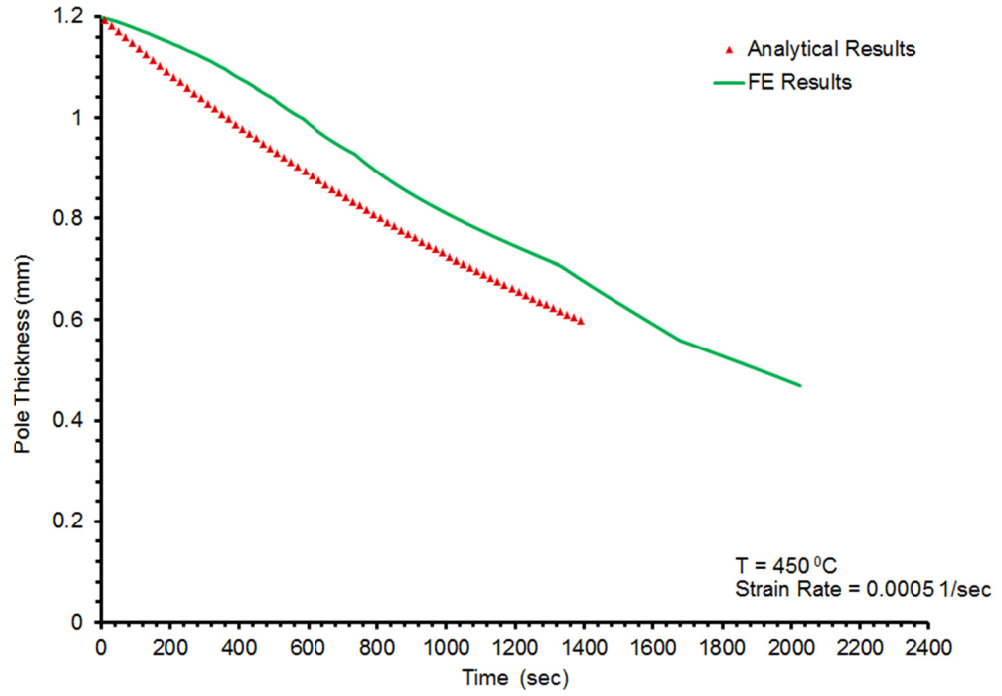

Figure 4. Dome pole thickness for AA5083 at 450 °C for FE model (solid line) and analytical results (triangles) (Dutta and Mukherjee, 1992)

3. Finite Element Analysis of the Single-Stage Superplastic Forming Process

The implicit code ABAQUS™/Standard was used to simulate the SPF of an AA5083 sheet into a practical part that has a complex geometry at 450 °C. The license plate pocket portion of an automobile decklid outer panel can be approximated to an infinitely long rectangular box, which allows for plane strain two-dimensional (2D) modeling of the mid-section of the license plate pocket.

3.1 Geometry and Model

The 2D model used for the simulation is presented in Figure 5. The model consists of an AA5083 sheet and a license plate pocket die. The sheet nodes at the left and right edges are constrained in the 1- and 2- directions (i.e. X- and Y- directions).

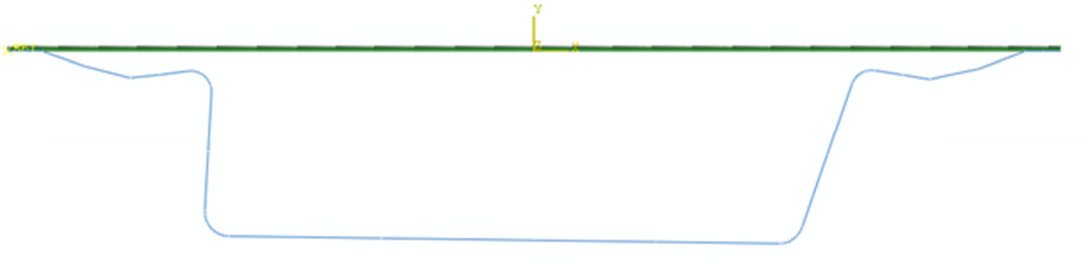

Figure 5. The 2D model used for the simulation of single-stage SPF

The AA5083 sheet used in this study has an original thickness of 1.2 mm. According to (Luckey, Friedman, & Xia, 2004), it was shown that 2D modeling using layered solid elements was more effective in predicting the thinning behavior than 3D modeling using conventional shell and membrane elements in SPF simulation. Since we are interested mainly in the thickness distribution of the final produced part, the AA5083 sheet was modeled using 4 layers of CPE4R elements. These are two-dimensional (2D), continuum, 4-node, reduced integration, plane strain elements. The mesh converged with 500 elements per layer.

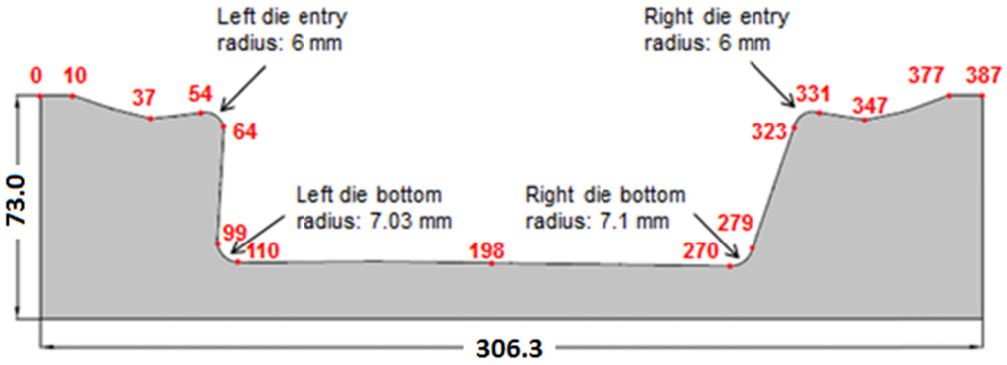

Figure 6. The die cross-section at the mid-section of the license plate pocket

Figure 6 shows the 2D model of the mid-section of the die used in the simulations. The details and dimensions of the die are taken from (Jarrar, Hector Jr., Khraisheh, & Bower, 2010). The horizontal dimension of the die is 306.32 mm. The lower left and right radii are 7.03 and 7.1 mm, respectively. The left and right die entry radii are both 6 mm. Note that the numbers in red represent the distance on the die surface starting from the upper left corner. The die was modeled as an analytical rigid surface. The analytical rigid surface gives better approximation to the physical contact constrain compared to element-based rigid surfaces, because it has the ability to parameterize the surface with curved line segments, which gives a smoother surface description (ABAQUS^{TM} User Manual, 2010).

The gas pressure profile was computed using an algorithm internal to ABAQUS^{TM} for maintaining a target strain rate of 0.001 1/sec. As a typical value used by other researchers such as (Albakri, Jarrar, & Khraisheh, 2011), a 0.2 coefficient of friction was used at the die-sheet interface in the FE simulations.

3.2 Predicted Pressure and Thickness Profile for the Single-Stage SPF

The forming of the license plate pocket ended when contact was established at all locations of the die. Figure 7 shows the computed gas pressure profile determined using the ABAQUS^{TM} built-in pressure control algorithm for maintaining a target strain rate of 0.001 1/sec. It is obvious from this figure that the ABAQUS^{TM} algorithm produces a step-wise curve. The reason for this is that the ABAQUS^{TM} algorithm allows for a wide tolerance range for the strain rate ratio (r). A detailed overview of this algorithm and other alternative algorithms can be

found in (Jarrar et a l., 2010) and (Jarrar, Hector Jr, Khraisheh, & Deshpande, 2012).We can also notice from Figure 7 that there is a sharp increase in the forming pressure at the final step in which the die corners were filled. The reason for this increase in forming pressure is that when the sheet touches the die at its sides and center, its resistance to forming increases, and thus a higher pressure is needed.

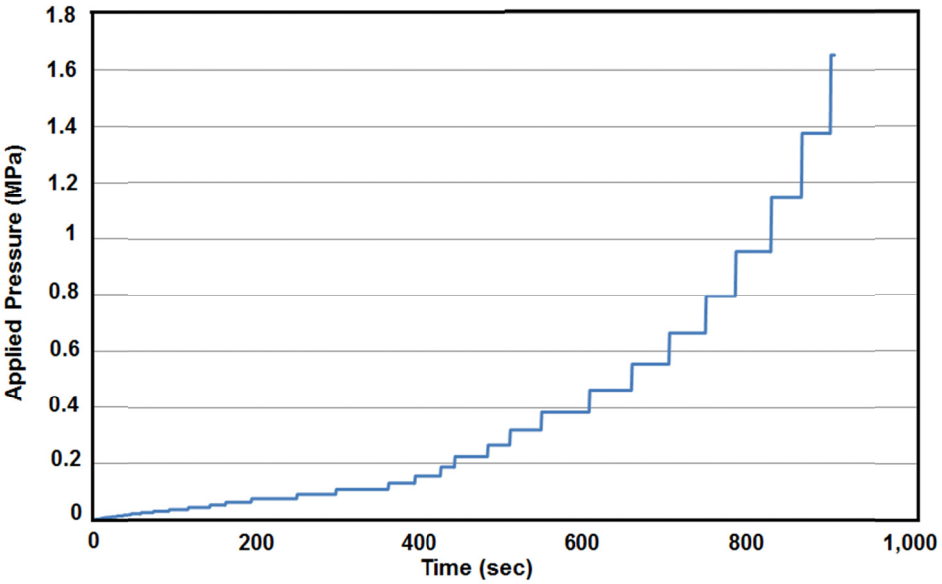

Figure 7. The FE computed gas pressure profile for a target strain rate of 0.001 1/sec using the build-in ABAQUS^{TM} algorithm

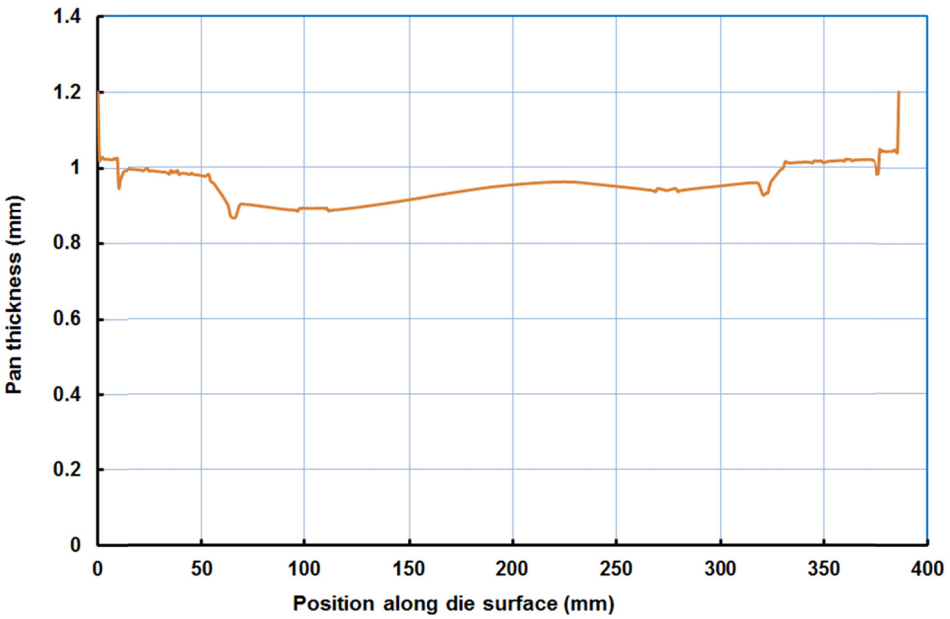

Figure 8. The FE predicted thickness profile at the mid-section of the formed license plate pocket

Figure 8 shows the FE predicted thickness profile at the mid-section of the formed license plate pocket using a target strain rate of 0.001 1/sec. It can be seen from this figure that the thickness distribution along the cross-section of the part is not uniform. The minimum thickness was noticed at the left entry radius. It was shown by (Jarrar et al., 2010) and (Albakri et al., 2011) that, for such geometry and coefficient of friction, the

entry radii of the part experience the most thinning due to the bending effects. On the other hand, thicker material distribution is found at the flange and center regions.

4. Finite Element Analysis of the Two-Stage Superplastic Forming Process

Two techniques were applied to improve the final thickness distribution of the superplastically formed component. The first technique is called reverse free bulging, in which the sheet to be formed was first blown away from the die, after producing a dome, the forming pressure was reversed forcing the bubble to take the shape of the die. The second technique is called sheet preforming, in which two gas pressure cycles were applied. In this approach, the model has two die cavities. During the first cycle the sheet was forced to take the shape of the upper die, after that, the forming pressure was reversed forcing the sheet to take the shape of the lower die which represents the final component cavity.

4.1 Reverse Free Bulging

The gas pressure was applied at the bottom of the AA5083 sheet in the first stage, which is the reverse free bulging stage. During this stage, the gas pressure profile was computed using an algorithm internal to ABAQUS^{TM} for maintaining a target strain rate of 0.001 1/sec. During the second stage, the forward SPF stage, the gas pressure was applied at the top of the AA5083 sheet, forcing it to take the shape of the license plate pocket die cavity under a constant strain rate of 0.001 1/sec.

The aim of the reverse bulging process is to pre-thin the superplastic sheet uniformly. This will minimize the possibilities of severe thinning and the early failure around the complex details of the die cavity (Nazzal, Zaid, & Al-Qawabah, 2011).

Two FE simulation runs were performed. For each simulation run, the superplastic sheet was bulged away from the die cavity to a preselected level during the first gas pressure cycle. Figure 9 shows the FE model used in the simulation for each case. Note that this figure displays the models after the free bulging stage. For the first case (part (a) from the figure) the AA5083 sheet was bulged away from the die cavity for 40 seconds, and in the second case (part (b) from the figure) it was bulged away for 80 seconds.

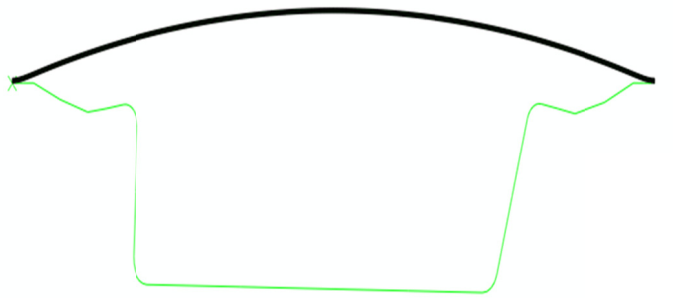

(a)

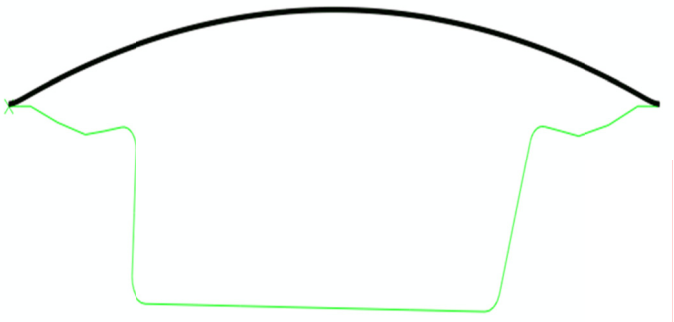

(b)

Figure 9. The 2D models after the reverse free bulging stage: (a) Case 1 (first stage time= 40 seconds), and (b) Case 2 (first stage time= 80 seconds)

4.2 Two-Stage SPF (Sheet Preforming)

The gas pressure was applied at the bottom of the AA5083 sheet in the first stage, which is the preforming stage. During this stage, the forming was performed under a constant gas pressure of 0.3 MPa. While during the second stage, the forward SPF stage, the gas pressure was applied at the top of the AA5083 sheet, forcing it to take the shape of the license plate pocket die cavity under a constant strain rate of 0.001 1/sec.

Based on the final thickness distribution of the 2D cross-section of the formed license plate pocket using the single-stage SPF, the preform die was designed to pre-thin the material in local regions that experienced the least thinning in the part cavity. As was discussed in section 3.2, for the process parameters considered, the entry radii of the geometry experienced the most thinning. Based on this finding, different preform dies were designed in a way to stretch the sheet at the flange and center of the cavity, where thicker material distribution was found using the single-stage SPF. Figure 10 presents four models used in sheet preforming. Each model consists of an AA5083 sheet, a preform die (upper die) and a license plate pocket die (lower die).

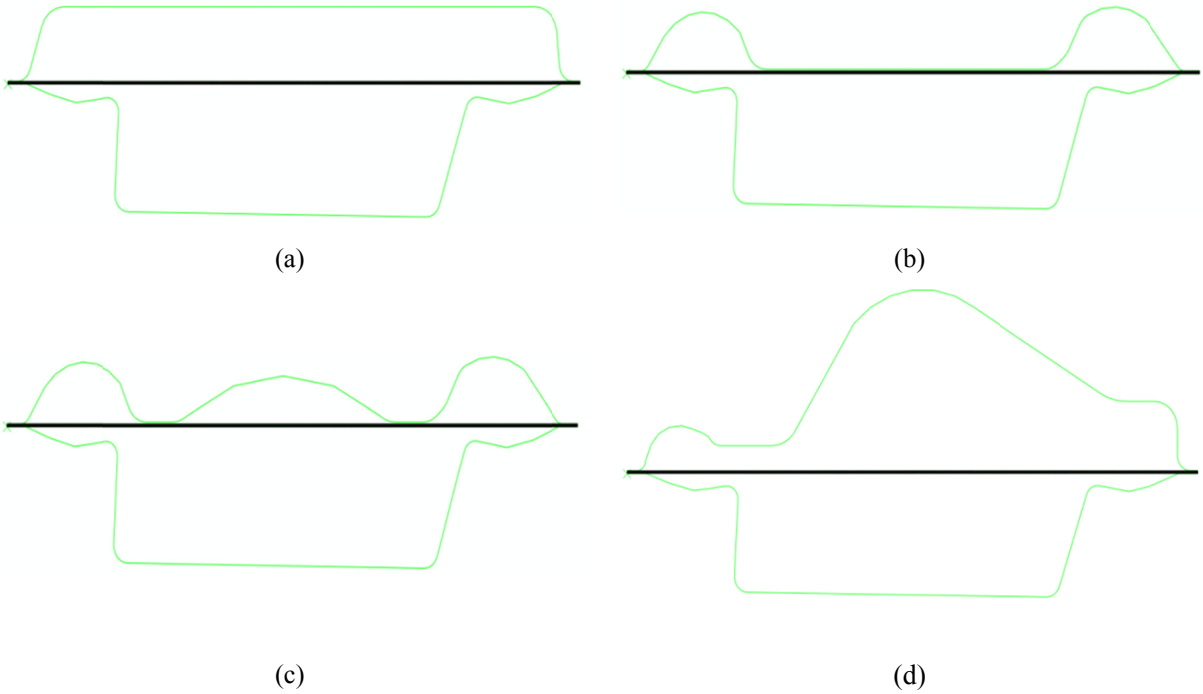

Figure 10. The 2D models used for the simulation of two-stage SPF: (a) Model 1, (b) Model 2, (c) Model 3, and (d) Model 4

The preform in part (a) from Figure 10 was designed to stretch the whole sheet, particularly at the flange region. In part (b), the preform cavity was designed to stretch the material only at the flange. A flat surface in the rest of the preform die cavity was used to keep the remaining regions unstretched and thus preserve the metal thickness in those regions during preforming. In part (c) the preform die cavity was designed to stretch the sheet at the center of the cavity and the flange regions, keeping the regions opposing the lower left and right entry radii and bottom corners without stretching. Finally, the last preform was engineered to pre-thin the sheet at all regions except the one opposing the left entry radius and bottom corner, the reason for not preforming this region is that it experienced the most thinning in the single-stage SPF.

5. Results and Discussion

Table 2 lists the forming time for each stage for the two cases of the reverse free bulging technique, along with the required forming time for the single-stage SPF. As expected, we can see from this table that the total forming time increased with increasing the duration of the reverse free bulging stage.

Table 2. Comparison in terms of forming time between the single-stage SPF and the two cases of reverse free bulging

	Forming Time (sec)		
	Reverse Free Bulging Stage	**Forward Forming Stage**	**Total**
Single-stage SPF	___	900.9	900.9
Case 1	40	938.5	978.5
Case 2	80	1000	1080

Figure 11 shows the computed gas pressure profile determined using the ABAQUS^{TM} built-in pressure control algorithm for maintaining a target strain rate of 0.001 1/sec, for each case along with the one for the single-stage SPF. Notice that the final pressure required for the single-stage SPF was 1.65 MPa. On the other hand, for cases 1 and 2, the final pressures required were 1.04 MPa and 1.09 MPa, respectively. Therefore, higher forming times and lower pressure values were required with the reverse free bulging method.

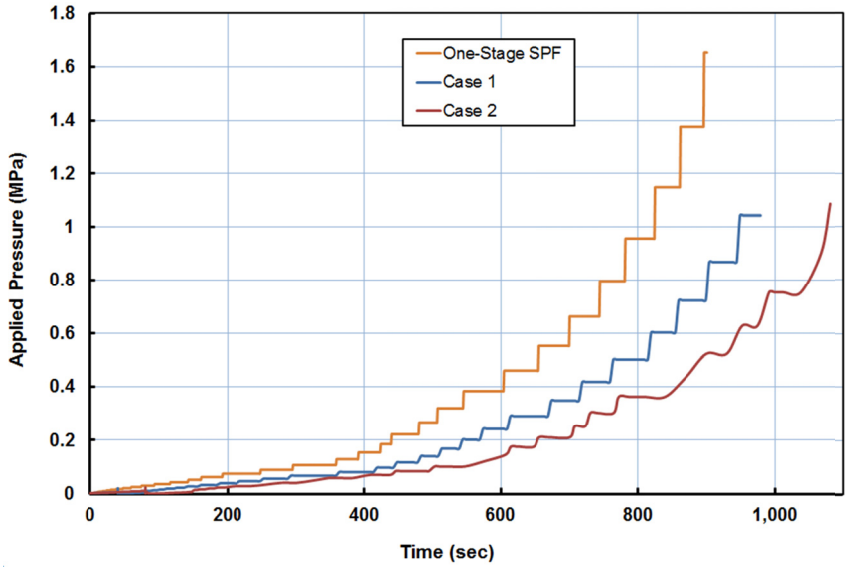

Figure 11. The FE computed gas pressure profiles for a target strain rate of 0.001 1/sec for the two cases of reverse free bulging compared with that for the single-stage SPF

The FE predicted thickness profile at the mid-section of the formed license plate pocket for each case compared with the thickness distribution obtained from the single-stage SPF is shown in Figure 12. It can be clearly seen from this figure that the reverse free bulging method resulted in almost the same thickness profile obtained from the single-stage SPF. The reverse free bulging technique only slightly increased the thickness at the entry radii. Table 3 shows the minimum and average thicknesses and the corresponding thinning factor obtained for each case. Note that the thinning factor, which is the ratio of the lowest thickness in the sheet to the average sheet thickness, was used as a quantitative measure of the uniformity of the thickness distribution of the formed part.

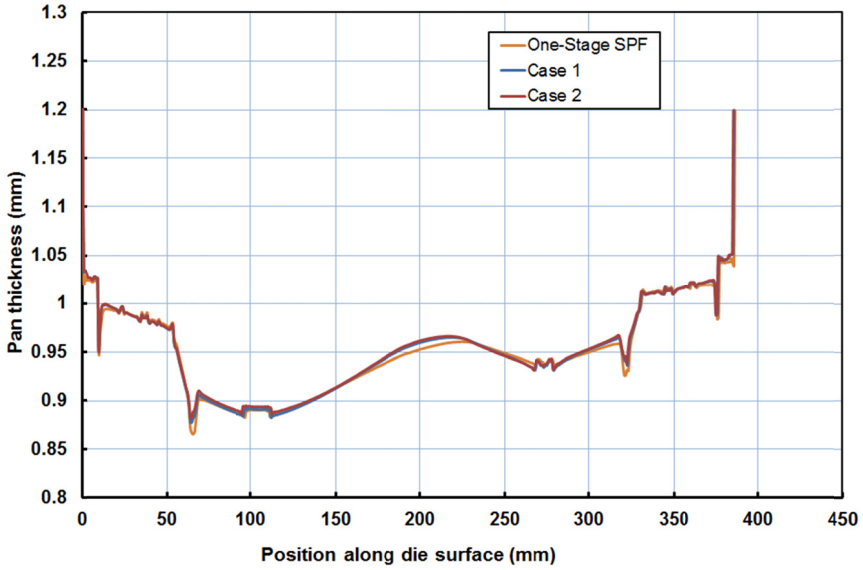

Figure 12. The FE predicted thickness profiles at the mid-section of the formed license plate pocket for the two cases of reverse free bulging compared with that from the single-stage SPF

Table 3 Comparison of the average and minimum thicknesses and thinning factor between the single-stage SPF and the two cases of reverse free bulging

	Minimum Thickness (mm)	Average Thickness (mm)	Thinning Factor
Single-stage SPF	0.86	0.96	0.9
Case 1	0.88	0.96	0.92
Case 2	0.88	0.96	0.92

Table 4 lists the forming time for each stage for the four models used in sheet preforming, along with the required forming time for the single-stage SPF. We can see from this table that, as expected, the total forming time required for the two-stage SPF was longer than that required for the single-stage SPF. The forming time required for the single-stage SPF was 900.9 seconds. Models 1, 2 and 3 required almost the same forming time, and model 4 required the longest forming time of 1351 seconds. Notice that the time required for the preforming stage of model 4 was longer than that for the forward forming stage. Also, the time required for the forward forming stage for all of the four models was shorter than that for the single-stage SPF.

Table 4 Comparison in terms of forming time between the single-stage SPF and the two-stage SPF using the four preform die models

	Forming Time (sec)		
	Preforming Stage	**Forward Forming Stage**	**Total**
Single-stage SPF	___	900.9	900.9
Model 1	391	800.1	1191
Model 2	351	800.1	1151
Model 3	351	700.1	1051
Model 4	801	550	1351

Figure 13 shows the FE generated gas pressure profile for each model, along with the one for the single-stage SPF. Note that the single-stage SPF was performed under a constant strain rate of 0.001 1/sec, and for two-stage SPF models, the first stage was carried out under a constant pressure of 0.3 MPa, and the second stage was under a constant strain rate of 0.001 1/sec. It can be seen from Figure 13 that there was a sharp increase in the forming

pressure at the final step for all of the models in order to fill in the bottom corners of the die. The reason for this increase in forming pressure is that when the sheet touches the die at its sides and center, its resistance to forming increases. The final pressure required for the single-stage SPF was 1.65 MPa. On the other hand, for models 1, 2, 3, and 4 the final pressure required was almost the same with a value around 1.3 MPa.

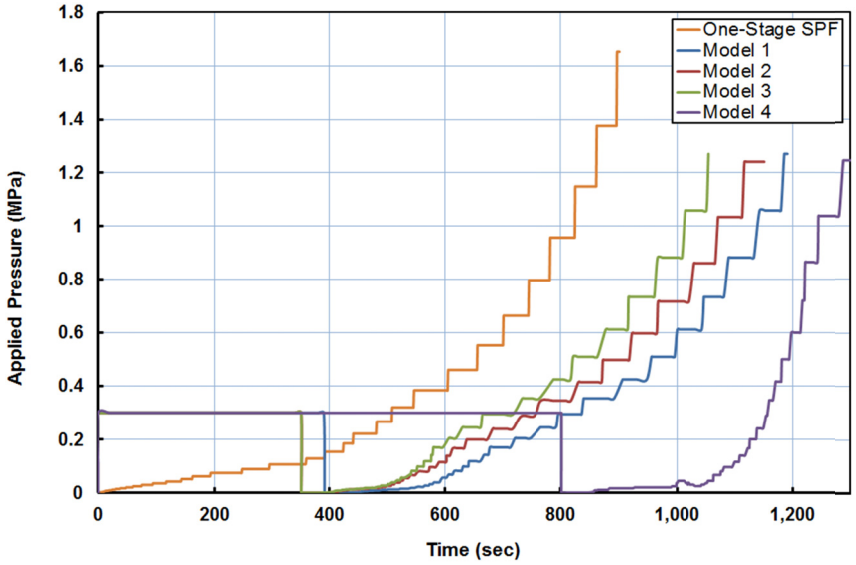

Figure 13. The FE computed gas pressure profiles for the single-stage SPF and the four models used for the two-stage SPF

The FE predicted thickness profile at the mid-section of the superplastic sheet for each of the four models after the preforming stage is shown in Figure 14. It can be seen from the figure that models 1, 2 and 3 made the sheet thicker at the center region, compared to the adjacent flange regions. This is due to the bulging at these regions during the preforming stage. While for the preform of model 4, which exhibited the most stretching, the sheet was pre-thinned at all regions to an almost uniform thickness distribution.

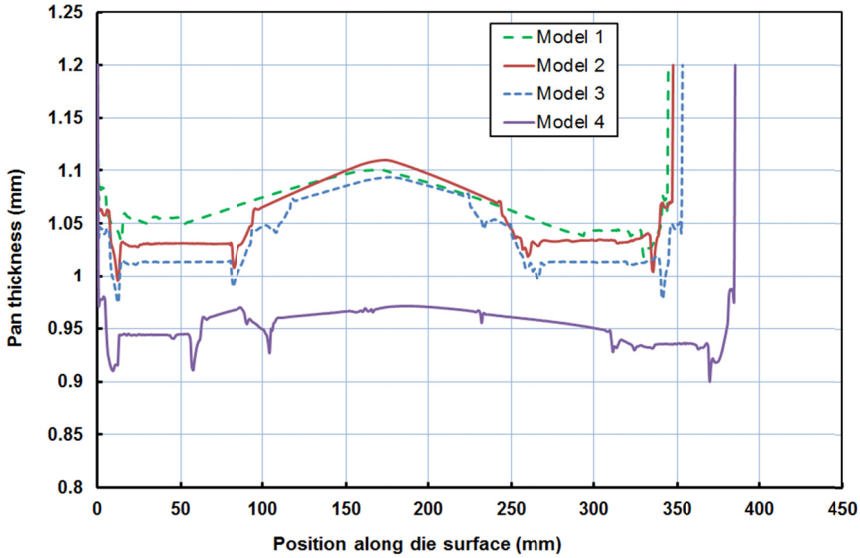

Figure 14. The FE predicted thickness profiles after the preforming stage of the four models.

The FE predicted thickness profile at the mid-section of the formed license plate pocket for each of the two-stage SPF models compared with the thickness distribution obtained from the single-stage SPF is shown in Figure 15. We can see that the four simulated models decreased the material thickness at the flange region. Models 1, 2 and 3 did not improve the thinning at the entry radii and the bottom corners. In addition, they increased the thickness at the bottom center of the cavity, which we want to decrease. This means that the center region needs extra stretching. In short, the first three models did not achieve a uniform thickness distribution. On the other hand, model 4 resulted in an almost uniform thickness distribution for the superplastically formed license plate pocket.

Table 5 compares the average and minimum thicknesses and the thinning factor values obtained for the single-stage SPF with that for the four models of the two-stage SPF. Model 4 increased the minimum thickness from 0.86 mm to 0.89 mm, which resulted in the highest increase compared to the rest of the models. Notice also that the thinning factor was decreased using models 2 and 3, and increased with models 1 and 4. The thinning factor was increased using the preform of model 4 from 0.9 to 0.94. In short, the best improvements in the minimum thickness and the thinning factor were obtained using the fourth model. The improvement in the minimum thickness was 3.5%, and for the thinning factor it was 4.4%. Figure 16 shows the predicted thickness profile for the single-stage SPF and the two-stage SPF (model 4), along with the thickness distribution obtained after the preforming stage of model 4. This figure shows how the engineered preform succeeded in improving the material distribution of the final part. It sacrificed some of the thickness at the flange and center regions in order to provide a better thickness at the entry radii and the bottom corners of the part.

Table 5. Comparison of the average and minimum thicknesses and thinning factor between the single-stage SPF and the two-stage SPF

	Single-stage SPF	Two-Stage SPF			
		Model 1	Model 2	Model 3	Model 4
Average Thickness (mm)	0.96	0.96	0.96	0.96	0.95
Minimum Thickness (mm)	0.86	0.87	0.86	0.85	0.89
Thinning Factor	0.9	0.9	0.89	0.89	0.94

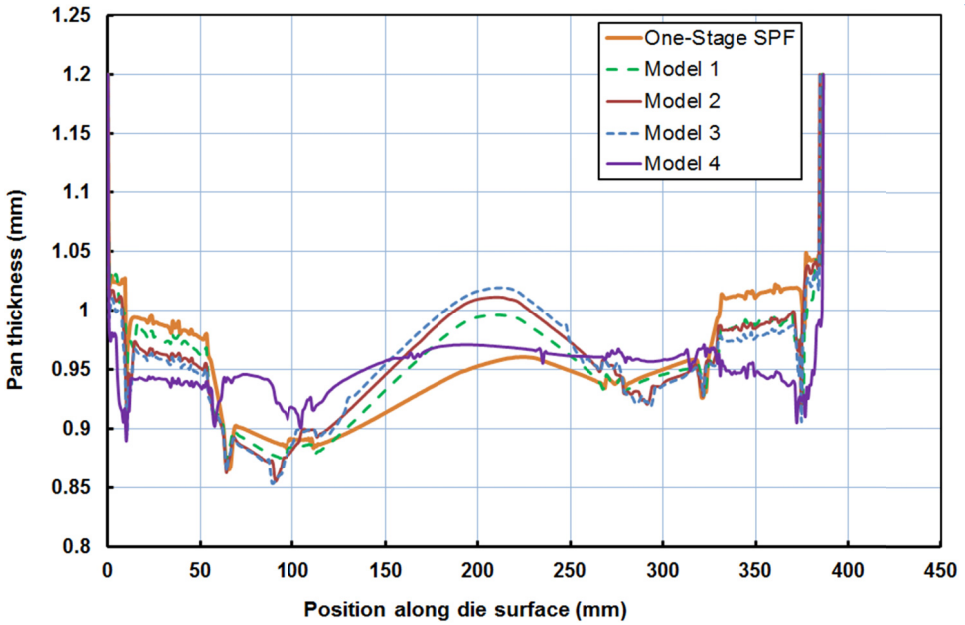

Figure 15. The FE predicted thickness profiles at the mid-section of the formed license plate pocket for the four models of the two-stage SPF compared with that from the single-stage SPF

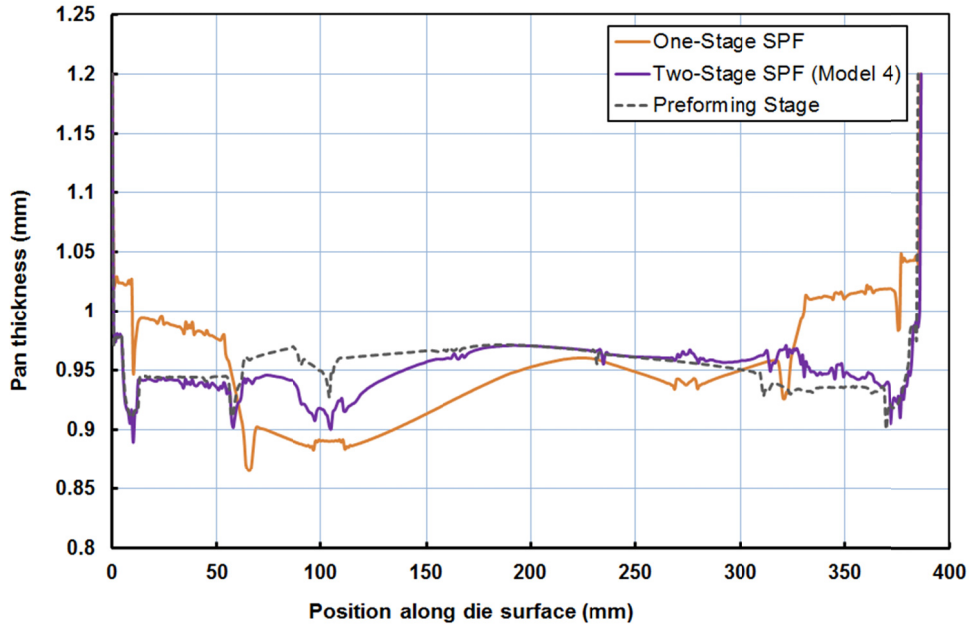

Figure 16. The FE predicted thickness profiles for the single-stage SPF and the two-stage SPF (Model 4) compared with that after the preforming stage

Finally, it is worth mentioning here that if the preform length of line exceeds the final part cross-section length of line, wrinkles would develop (Luckey et al., 2009). As can be seen in Table 6, the length of line for the preform cross-section of model 4 was 381.6 mm, and for the license plate pocket cross-section it was 387.9 mm. This means that the length of line of our designed preform did not exceed the final formed part length of line.

Table 6. Comparison of the cross-section length of line for the license plate pocket and that of the preform of model 4

Preform Length of Line, $L_{preform}$ (mm)	381.6
Part Length of Line, L_{part} (mm)	387.9
$L_{preform}/L_{part}$ (%)	98.4

6. Conclusions

A power creep law material model fit to tensile data over a wide range of strain rates was developed and used as an input to the commercial FE code, ABAQUS™. The model was used in simulating bulge forming of AA5083 under SPF conditions. The predicted pole height and thickness evolution profiles were compared with experimental and analytical results. The developed constitutive model led to FE predictions that follow the experimental and analytical trends.

The implicit code ABAQUS™/Standard was used to simulate the single-stage SPF of an AA5083 sheet into a practical part that has a complex geometry at 450 °C. The SPF process was carried out under a constant strain rate of 0.001 1/sec. The FE predicted thickness profile showed a non-uniform thickness distribution. An excessive thinning was noticed at the entry radii and the bottom corners of the part. On the other hand, thicker material distribution was found at the flange and center regions of the cavity.

Two techniques were applied to improve the final thickness distribution of the formed license plate pocket; reverse free bulging and sheet preforming. The study concluded that the total forming time increased with increasing the duration of the reverse free bulging stage. In addition, this method resulted in almost the same thickness profile obtained from the single-stage SPF, hence, did not achieve our main goal for this work.

Four preform die designs were presented for the sheet preforming technique. Gas pressure and thickness profiles for each design were compared with that of the single-stage SPF. The fourth model, which exhibited the most

stretching, required the longest forming time of 1351 seconds. The first three models did not achieve a uniform thickness distribution. On the other hand, the fourth model resulted in an almost uniform thickness distribution for the superplastically formed part. The improvement in the minimum thickness was 3.5%, and in the thinning factor it was 4.4%. In order to achieve a wrinkle-free component, the preform length of line was calculated to ensure that it did not exceed the final part cross-section length of line.

References

ABAQUS™. (2010). *Analysis user's manual*. version 6.10.

Abu-Farha, F., & Nazzal, M. (2010). Advancing elevated temperature hydro/pneumatic sheet metal forming operations through reverse bulging. *Transactions of the NAMRI/SME*, *38*, 601-608.

Albakri, M. I., Jarrar, F. S., & Khraisheh, M. K. (2011). Effects of interfacial friction distribution on the superplastic forming of AA5083. *Journal of Engineering Materials and Technology*, *133*(3), 031008-031014. http://dx.doi.org/10.1115/1.4004159

Bradley, J. R. (2004). Bulge testing of superplastic AA5083 aluminum sheet. In E. M. Taleff, P. A. Friedman, P. E. Krajewski, R. S. Mishra, & J. G. Schroth (Eds.), *Advances in Superplasticity and Superplastic Forming* (pp. 109-118), Charlotte, North Carolina, USA.

Dutta, A., & Mukherjee, A. K. (1992). Superplastic forming: An analytical approach. *Materials Science and Engineering: A*, *157*, 9-13. http://dx.doi.org/10.1016/0921-5093(92)90092-F

Fischer, J. R. (1998). *Prethinning for superplastic forming*. U. S. Patent number 5823032.

Jarrar, F. S., Hector Jr, L. G., Khraisheh, M. K., & Bower, A. F. (2010). New approach to gas pressure profile prediction for high temperature AA5083 sheet forming. *Journal of Materials Processing Technology*, *210*(6), 825-834. http://dx.doi.org/10.1016/j.jmatprotec.2010.01.002

Jarrar, F. S., Hector Jr, L. G., Khraisheh, M. K., & Deshpande, K. (2012). Gas pressure profile prediction from variable strain rate deformation paths in AA5083 bulge forming. *Journal of Materials Engineering and Performance*, *21*(11), 2263-2273. http://dx.doi.org/10.1007/s11665-012-0196-1

Jarrar, F., Liewald, M., Schmid, P., & Fortanier, A. (2014). Superplastic forming of triangular channels with sharp radii. *Journal of Materials Engineering and Performance*, *23*(4), 1313-1320. http://dx.doi.org/10.1007/s11665-014-0878-y

Johnson, W., Al-Naib, T. Y. M., & Duncan, J. L. (1972). Superplastic forming techniques and strain distributions in a zinc-aluminum alloy. *Journal of the Institute of Metals*, *100*, 45-50.

Jovane, F. (1968). An approximation analysis of the superplastic forming of a thin circular diaphragm: Theory and experiments. *International Journal of Mechanical Sciences, 10*, 403-427. http://dx.doi.org/10.1016/0020-7403(68)90005-2

Kleiner, M., Geiger, M., & Klaus, A. (2003). Manufacturing of lightweight components by metal forming. *CIRP Annals - Manufacturing Technology*, *52*(2), 521-542. http://dx.doi.org/10.1016/S0007-8506(07)60202-9

Krajewski, P. E., & Montgomery, G. P. (2004). Mechanical behavior and modeling of AA5083 at 450C. In E. M. Taleff, P. A. Friedman, P. E. Krajewski, R.S. Mishra, & J.G. Schroth (Eds.), *Advances in Superplasticity and Superplastic Forming* (pp. 341-350), Charlotte, North Carolina, USA.

Lan, H., Fuh, Y., Lee, S., Chu, C., & Chang, T. (2013). Two-stage superplastic forming of a V-shaped aluminum sheet into a trough with deep and irregular contour. *Journal of Materials Engineering and Performance, 22*(8), 2241-2246. http://dx.doi.org/10.1007/s11665-013-0511-5

Luckey, S. G., Friedman, P. A., & Weinmann, K. (2009). Design and experimental validation of a two-stage superplastic forming die. *Journal of Materials Processing Technology, 209*, 2152-2160. http://dx.doi.org/10.1016/j.jmatprotec.2008.05.019

Luckey, S. G., Friedman, P. A., & Xia, Z. C. (2004). Aspects of element formulation and strain rate control in the numerical modeling of superplastic forming. In E. M. Taleff, P. A. Friedman, P. E. Krajewski, R. S. Mishra, & J. G. Schroth (Eds.), *Advances in Superplasticity and Superplastic Forming* (pp. 371-380), Charlotte, North Carolina, USA.

Nakamura, K. (1989). Manufacturing method of formed product having required wall thickness by superplastic blow forming method. Patent abstract of Japan No. 197020.

Nazzal, M., Zaid, A., & Al-Qawabah, S. (2011). Finite element simulation of a hybrid forming process: Deep drawing and superplastic forming. In *Proceedings of the 21st International Conference on Production Research*, Stuttgart, Germany.

Pilling, J., & Ridley N. (1989). *Superplasticity in crystalline solids*, London: The Institute of Metals.